PANCHAKOTesSAYS
ISSN : 0976-4968
Vol-15, No.-1, May 2024

Study of Electrical Properties of Methylammonium Bismuth Bromide Nanoparticles

Arup Dhara

Department of Physics, Burdwan Raj College, Burdwan, West Bengal-713104, India; Email: *arupdhara2010@gmail.com*

Abstract

Methylammonium Bismuth Bromide ($CH_3NH_3)_3Bi_2Br_9$ has been successfully synthesized by mechano-chemical method. It is a Lead free hybrid halide perovskite material and may be a good alternative for Pb based perovskites for the applications of photovoltaic cell. The formation, crystallinity and quality of the sample are confirmed by the XRD pattern and PL spectrum. Temperature-dependent electrical and dielectric properties have been investigated in detail.

KEYWORDS: Lead free hybrid perovskite, Dielectric properties, Impedance spectroscopy.

INTRODUCTION

Global demand of energy is increasing rapidly due to ever-growing population. Renewable energy is the most viable solution to fulfill this demand as well as to prevent environmental degradation. There are broadly two types of renewable energy namely “On-grid” and “Off-grid”. Photovoltaic module belongs to the “off-grid” renewable energy. In recent years, Perovskite solar cell (PSC) emerged as a most promising third-generation photovoltaic technology for its high-performance, eco-friendly with a high power conversion efficiency (PCE) of more than 25%, indicating a great potential application for future [1-3]. Lead halide perovskite materials have been paid great scientific attention in the field of optoelectronics due to their attractive properties like direct band gap, strong optical absorption coefficient, high charge carrier mobility, long charge carrier lifetime and long diffusion length. Apart from these features, they do posses high open circuit voltages caused by photon recycling; as a consequence they have long charge extraction length through multiple absorption-emission events within the perovskite active layer [4-6]. Due to these features, the lead halide perovskites have been observed to demonstrate an increase in power conversion efficiency (PCE) from 2% to 25 %. Behind this performance, the metal Pb plays a crucial role for its intrinsic properties like high melting point, high density, corrosion resistance, ductility etc. In spite of these advantages, with lead based perovskites concerns remain about the materials toxicity and stability. These serious issues forced the scientific society to think about an alternative one with the similar type properties. Therefore it has been necessary to address these issues by replacing the lead metal with a nontoxic element. Methyl

ammonium lead halide based perovskites ($CH_3NH_3PbX_3$: X=I,Cl,Br) have drawn a great attention of the research community for its merits in versatile applied fields such as opto-electronic and photovoltaic applications. Bi may be a suitable replacement of Pb due its close position in the periodic table. Because it has similar ionic radius and electronic structure with Pb^{2+}, it can be expected to be similar optoelectronic properties**.** Due to the similar ionic radius of Bi^{3+} ion with Pb^{2+}, it is expected to substitute the position of the Pb^{2+} ions in the perovskite crystal structure [7-9]. In this paper, we have studied the electrical properties of $(CH_3NH_3)_3Bi_2Br_9$ (MABB).

MATERIALS AND METHODS

To synthesize Methylammonium Bismuth Bromide [$(CH_3NH_3)_3Bi_2Br_9$], we have used Methylamine Bromide [$CH_3NH_2Br_3$], Bismuth Bromide [$BiBr_3$, Sigma Aldrich, 99%], Dimethylformamide (DMF) [C_3H_7NO, Merck Chemicals, 99.5%] Toluene [Merck Chemicals]. All the chemicals were of analytical grade and used without any further purification. Initially, Methylammonium Bromide (MABr) powder was synthesized via a wet chemical route. Then, MABr and $BiBr_3$ powders were hand grinded in an agate mortar for 30 min to obtain a homogeneous mixture. The mixture was then transferred to a stainless steel vial of 100 ml volume containing stainless steel balls having the ball to powder mass ratio 40:1. Milling of the powder mixture was performed in a planetary ball mill (Gaelon enterprise, China) for six hours at 500 RPM with subsequent pause of milling after every 5 min to avoid contamination from the milling media. After the six hour milling process, the material was collected incolloidal form which was then dried in vacuum at 50 ^{0}C to evaporate the milling medium. Thus, the synthesized material was obtained in the powder form and used for XRD and electrical measurements.

For the electrical measurements, synthesized powdered samples were pressed under a hydraulic press at 500 MPa to form pellet of 13 mm diameter and almost 1 mm thickness. To prepare the pellet for good electrical contacts, two copper strip of the same diameter were used from both surface of the pellet. All samples are preheated up to 600K and electrical measurements are carried out by conventional two probe method during cooling. The ac electrical measurement is carried out using the LCR meter (IM3536 HIOKI) in the temperature range 333K-453K and frequency range 4 Hz-1MHz.

RESULTS AND DISCUSSION

XRD patterns of the synthesized powder MABB obtained by ball-milling of AX_3 and BiX_3 (A= CH_3NH_2, X= Br) in Fig.1 (a). The several peaks in the XRD pattern confirms the

crystalline nature of the synthesized material and the XRD peaks do not match with the peak of the constituent materials which confirms the formation of new material after milling. The XRD peaks are in good agreement with the published Inorganic Crystal Structure Database (ICSD) [10].

The room temperature PL spectra of MABB has been recorded in the wavelength range 390 nm- 730 nm at an excitation wavelength 325 nm. The PL spectrum is shown in Fig.1b. The high PL intensities further support the formation of good quality sample. In Fig.1 (a), we observe two distinct emission peaks around 465 nm (≈2.67 eV) and 480 nm (≈2.59 eV) in the green and orange region respectively. The green emission occurs due to transition from conduction band to V_o level [11]. The reduced intensity excitonic peak around 540 nm is a good indication of loosely bound excitons compatible with large crystallites.

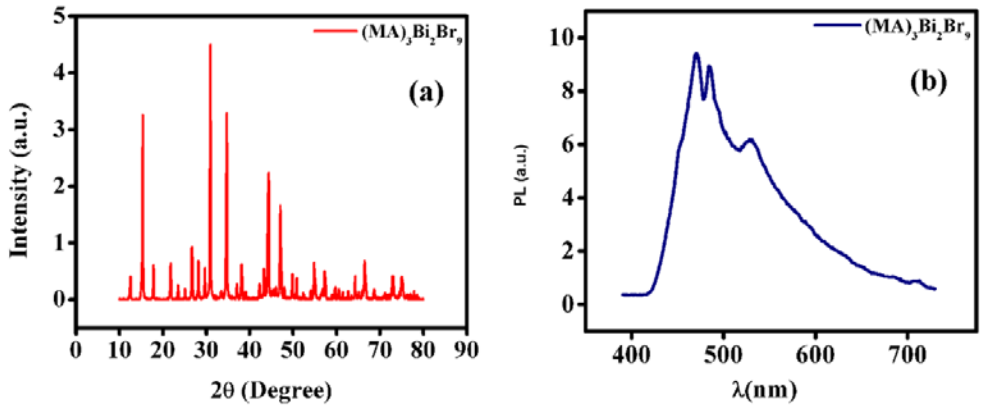

Fig.1: (a) XRD pattern (b) PL spectrum of MABB

The complex impedance plane plots Z'' vs Z' of $[(CH_3NH_3)_3Bi_2Br_9]$ is shown in Fig.2. For the analysis of the experimental data, the curves are fitted with Z-view software to an equivalent circuit composed of a series array of two sub-circuits. Where (R_g, R_{gb}) and (C_g, C_{gb}) are the resistances and capacitances of grains and grain boundaries, respectively. As polycrystalline material generally shows grain boundary impedances [12-13]. In this equivalent circuit model, there are mainly two distorted semicircles, the first one represents grains effect (high-frequency region) and the second semicircle represents grain boundaries (low-frequency region). No other relaxation process, such as sample-electrode interface effects, could be observed through this formalism in the applied frequency and temperature range. The radii of the semicircles decrease with increasing temperatures, indicating the semiconducting behavior of the material. The center of the semicircles lies just below the real

impedance axis, which indicates the presence of non-Debye type relaxation process in the material.

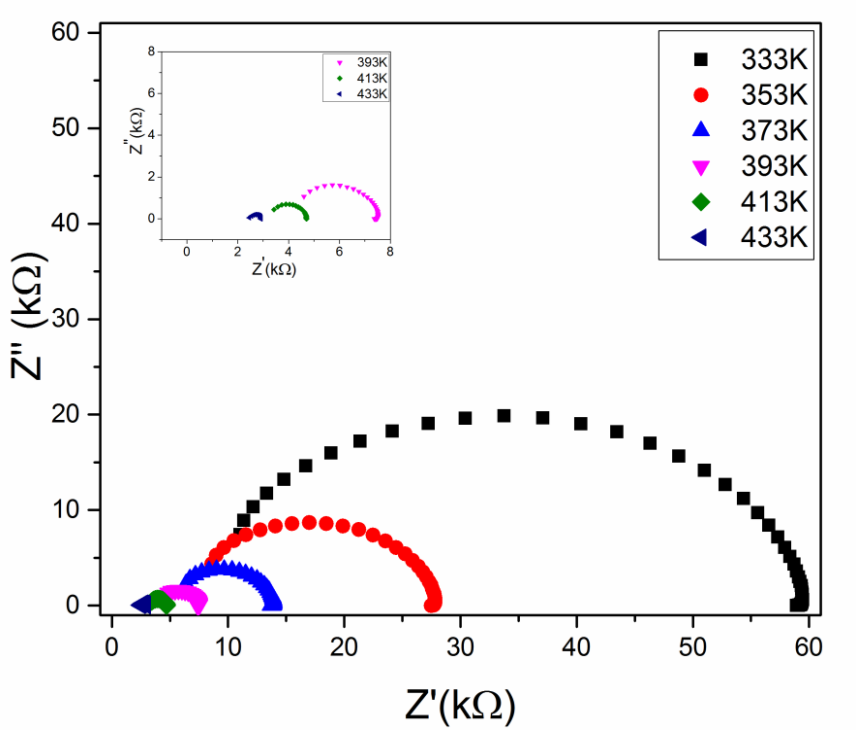

Fig.2: Cole-Cole plots of MABB at different temperatures

A material reflects its dielectric properties when an external field is applied to this material. Fig.3 shows the variations of dielectric constant (ε') with respect to the applied frequency at different temperature of the surrounding environment of MABB. The value of ε' showed an upward tendency in the temperature range from 333K to 433K. It is clear from the Fig.3 that the material follows the external field up to ~ 100 Hz (resonance frequency of the material), after that the dielectric constant become independent of the applied frequency at all measured temperature.

The reason behind the trend is based on Maxwell-Wagner polarization mechanism. In this mechanism, at the frequency higher than the resonance frequency, less space charge are accumulated at the grain boundary region and consequently minimizes the dielectric losses.

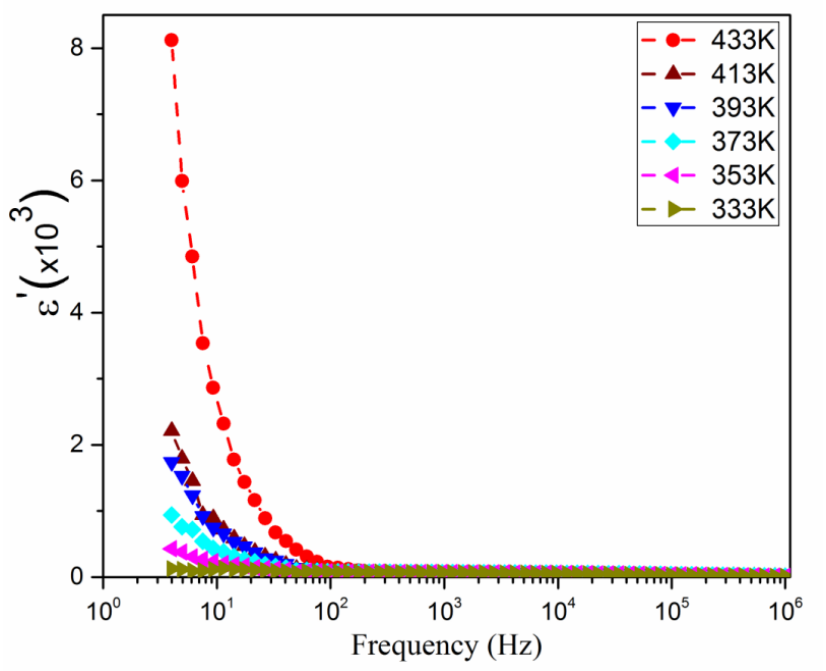

Fig.3: Frequency variation of real part (ε') of complex dielectric constant(ε^*) of MABB at different temperatures.

CONCLUSION

In the present study, lead free hybrid halide perovskite $(CH_3NH_3)_3Bi_2Br_9$ has been synthesized by mechano-chemical technique. Temperature and frequency dependent electrical and dielectric properties have been studied extensively. The complex impedance spectroscopy study confirms the semiconducting nature of the sample. Thus, the finding results indicate that the material may be a good alternative lead free material for photovoltaic applications.

ACKNOWLEDGEMENTS

The author wishes to thank to Dr. Sachindranath Das, Jadavpur University, for allow me to access his laboratory.

REFERENCES

1. P. Mahajan, R. Datt , W. Chung Tsoi , V. Gupta , A. Tomar, S. Arya, *Coord. Chem. Rev.*,429, 213633 (2021).
2. S. K. Sahoo, B. Manoharan, and N. Sivakumar, *Introduction: Why Perovskite and Perovskite Solar Cells?* (Elsevier Inc., 2018).
3. A. Aftab and M. I. Ahmad, *Solar Energy* 216, 26 (2021).
4. D. D. Smith, P. Cousins, S. Westerberg, R. De Jesus-Tabajonda, G. Aniero, and Y. C.

Shen, *IEEE Journal of Photovoltaics* 4, 1465 (2014).
5. S. Patwardhan, D. H. Cao, S. Hatch, O. K. Farha, J. T. Hupp, M. G. Kanatzidis, and G. C. Schatz, *Journal of Physical Chemistry Letters* 6, 251 (2015).
6. N. J.Jeon, J. H. Noh, W. S.Yang, Y. C. Kim, S. Ryu, J. Seo, S.I. Seok; *Nature 517;*476–480(2015).
7. A.Kojima, K.Teshima, Y. Shirai, T. Miyasaka; *J. Am. Chem. Soc. 131 (17),* 6050–6051(2009).
8. C A López, M C Alvarez-Galván, M V Martínez-Huerta, F Fauth, J A Alonso; *CrystEngComm ,22,* 767 (2020)
9. M. M.Lee, J. Teuscher, T. Miyasaka, T. N. Murakami, H.J. Snaith; *Science 338;* 643–647 (2012).
10. T. Paul and A. Ghosh, *J. Appl. Phys. 121*, 135106 (2017).
11. C. H. Ahn, Y.Y. Kim, D.C. Kim, K. Mohanta, and H. K. Cho, *J. Appl. Phys.* 105 (2009) 013502.
12. N.H. Vasoya, P.K. Jha, K.G. Saija, S.N. Dolia, K.B. Zankat, and K.B. Modi, *J. Electron. Mater. 45*, 917 (2016).
13. W. Zhu, C. Bao, F. Li, T. Yu, H. Gao, Y. Yi, J. Yang, G. Fu, X. Zhou, Z. Zou;*Nano Energy 19,* 17–26(2016).